GE Oil & Gas

Leonardo Nettis, GE Oil & Gas
Enzo Imparato, GE Oil & Gas
Lorenzo Cosi, GE Oil & Gas

DOWNSTREAM TECHNOLOGY SOLUTIONS | PRODUCTS & SERVICES

Enhancement of a large injection system for steam turbines

Abstract

Steam turbines operate in production plants where there are very large injections of low-pressure steam. That's why the injection system must be designed and enhanced for efficient turbine performance and uniform flow at the inlet of the low-pressure stages downstream from the injection.

GE Oil & Gas illustrates the enhancement of a steam turbine injection system on a unit in which injection flow is 80 percent of the total outlet mass flow. In this process, the shape of the original steam guide was varied to reduce the total pressure loss and make the circumferential flow distribution uniform.

The analysis used RANS 2D and 3D-CFD solver. The design process had three different steps:

- Axisymmetric CFD screening based on DOE
- 3D-CFD verification of the profile shape previously obtained, with the additional estimation of the flow uniformity on 360°
- 3D-CFD analysis of the injection module, including the reaction stage upstream and the first LP stage downstream, with the stator modeled on 360°

The main outcomes are presented in terms of total pressure loss and uniformity of circumferential flow—both of which were strongly reduced from the original design's yields. An analysis in the frequency domain of the flow distribution also has been performed to characterize the excitation associated with flow non-uniformity.

Introduction

Demand is constantly increasing for industrial steam turbines that are reasonably efficient even when a large injection of steam is present. That's because there are many different applications for that kind of turbine. To better accommodate the injection in these applications without compromising steam turbine performance in power generation, use a steam guide in the section between the HP and LP stages, where the injection occurs, to simultaneously reduce total pressure losses and flow non-uniformity.

The solution has been evaluated by a CFD-RANS-based numerical analysis. Similar test cases have been studied and validated with the same approach by Schramm et al. [1] and Engelmann et al. [2]. Here is how the work was structured:

- A preliminary assessment of the steam guide was conducted by 2D axisymmetric analysis to investigate a large DOE without extremely time-consuming simulations.
- Several axisymmetric solutions were selected and simulated in 3D to determine how much they could reduce non-uniformity. The 3D model also simplifies the stator downstream, which is described later.
- The final best solution, arising from the previous comparison, was simulated together with the reaction stage upstream and the LP stage downstream, with the stator blade row modeled on 360°.

Finally, the impact of the steam injection on the LP rotor downstream was studied by computing the excitation in the frequency domain.

The next section introduces the steam flow conditions for the main flow and the injection, together with the domain geometry.

Nomenclature

CFD	Computational Fluid Dynamics
DOE	Design Of Experiment
FFT	Fast Fourier Transform
HP	High Pressure
HT	Total Enthalpy
IAPWS	International Association for the Properties of Water and Steam
LP	Low Pressure
M	Mass Flow Rate
NPF	Nozzle Passing Frequency
PS	Static Pressure
RANS	Reynolds Averaged Navier-Stokes
REV	Revolution
RPM	Revolution Per Minute
Y+	Non-Dimensional Wall Distance

Greek Symbols

ϕ	Diameter
θ	Angle

Super- and Subscripts

AS	Axisymmetric
Ave	Average
Inj	Injection
Main	Main Flow

Problem formulation

As previously mentioned, and depicted in Figure 1, the global domain being analyzed has a reaction stage followed by the injection system and, lastly, the LP stage downstream. The main features of both stages, along with the operating conditions at the design point, are listed in Table 1.

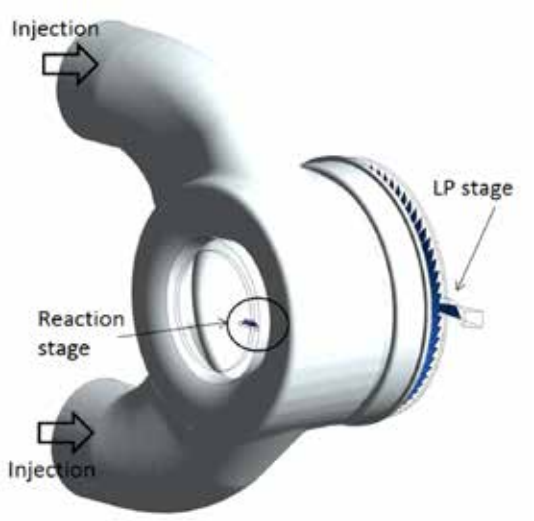

FIGURE 1 Global computational domain

REACTION STAGE		
Stator Blade Count		126
Rotor Blade Count		126
Reaction degree		50%
LP STAGE		
Stator Blade Count		70
Rotor Blade Count		56
OPERATING CONDITIONS		
RPM		**3207**
Reaction Stage Inlet	Pressure [barA]	0.57
	Temperature [°C]	84.6
Injection	Pressure [barA]	0.5
	Temperature [°C]	81

Table 1 Turbine stage geometry and operating conditions at design point

The realistic geometry previously shown corresponds to the last phase of this study, namely the computational domain used for the best solution. The only approximation pertains to the cavities that have not been modeled for rotor and stator blades.

However, the impact of the consequent leakages is considered to be negligible for the scope of this work.

Starting from this domain, the following simplifications were realized:

- Simplified 3D model, Figure 2: The main difference is a convergent duct in place of the LP stator blade row. This creates the same area reduction and also drastically lowers the grid size for the full blade row. Moreover, there is no reaction stage upstream, but the main inlet corresponds directly to the stage rotor outlet.
- Axisymmetric model, Figure 3: The 3D model with the convergent duct was further simplified by making it axisymmetric. Obviously, the injection inlet was treated as an axisymmetric inlet, although it is not, with the same circumferential angle °AS. However, the proper boundary conditions were imposed to keep the same proportionality between the two mixing flows, as better explained in the setup phase.

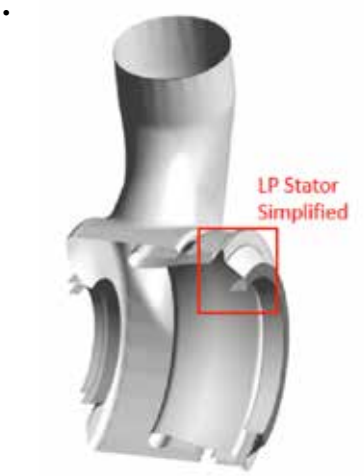

FIGURE 2 3D simplified model: convergent duct highlighted

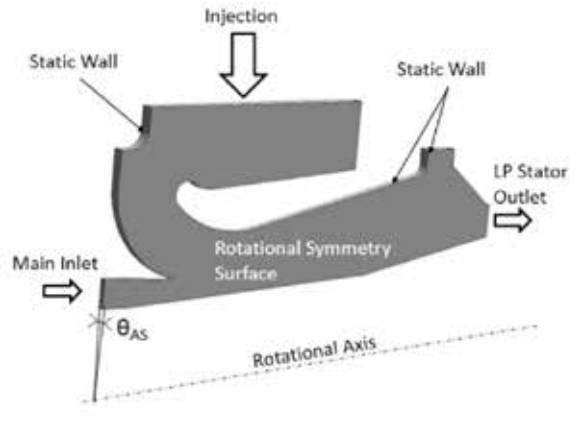

FIGURE 3 Axisymmetric model

Methodology

Meshing approach

The complete domain—the one including blade rows—has been discretized through the following two approaches:

- **Injection domain:** An ANSYS® internal mesher performed the meshing process, while a hybrid grid comprised of tetrahedra and prisms was realized and used for the boundary layer region. The same approach was employed for simplified and complete models. Grid independence analysis was performed on the simplified version of the enhanced configuration, as later described.
- **Blade row:** The Autogrid* [3] tool performed the mesh generation. The preferential kind of elements for this typology of domain, hexahedra, was adopted.

To obtain y+ close to 1, a common set of parameters was used for these two tools in proximity to the wall; this is summarized in Table 2.

Finally, mixing planes were used, in the complete test case, between rotating and stationary domains. The direct matching is present only between the injection domain and the LP stator downstream, with a simple interpolation of the aerodynamic quantities on 360°, instead of a further averaging process that would compromise the circumferential non-uniformity, here under analysis. A similar cell size was adopted on both sides of the interface to improve the interpolation between injection and LP stator domains.

MESH PARAMETERS		
Height of first layer [mm]		1E-5
Cell expansion ratio		1.2
Number of layers		25
Total Number of Cells (Millions)	Realistic	70
	Simplified 3D	20
	Axisymmetric	0.5

Table 2 Mesh parameters for the computational domain

Numerical model (CFD)

Because of the good compromise between accuracy and computational time required for 3D complex geometries, the most commonly employed approach in the turbomachinery field to numerically solve the Navier-Stokes equations is the Reynolds Averaged Navier-Stokes (RANS). In particular, the commercial software ANSYS® CFX® [4] has been used to solve the steady state simulations under consideration. The IAWPS steam tables, available in the code, were employed to properly model the fluid properties.

Turbulence modeling: The SST k-ω two-equations model, first introduced by Menter [5], and widely tested in similar turbomachinery applications (see [1] and [2]), was used to model turbulence. In ANSYS® CFX®, this model is associated with the automatic near wall treatment, where a smooth transition between a low Reynolds number approach (y+ < 5) and standard wall functions (y+ > 30) is adopted in the range between these y+ values (see Menter et al [6]). However, due to the low value of y+ achieved with the grids employed in this work, this treatment corresponds to the low Reynolds model, where the viscous sub-layer is not modeled but directly solved.

Boundary conditions: The scheme of the BCs imposed in each model is shown hereafter. In particular, the axisymmetric and the 3D simplified domains share the same set of conditions. The mass-flow rate m_{inj} imposed in the axisymmetric case corresponds to the real injection flow rate rescaled on the angle θ_{AS}.

FIGURE 4 Boundary conditions scheme

On the other hand, similar BCs have been adopted for the analysis where stages are included, but obviously they differ according to the location where they are imposed. The total enthalpy at the inlet is relative to the reaction stage inlet, and the average static pressure at the outlet corresponds to the LP rotor outlet value. The different conditions imposed are well summarized in Table 3.

BOUNDARY CONDITIONS			
Axisymmetric and 3D simplified	Main Inlet (Reaction stage outlet)	M [kg/s]	8.9
		HT [kJ/kg]	2653
	Injection	M [kg/s]	30.9
		HT [kJ/kg]	2647
	Outlet (LP stator outlet)	PS [barA]	0.23
3D realistic	Main Inlet (Reaction stage inlet)	M [kg/s]	8.9
		HT [kJ/kg]	2645
	Injection	M [kg/s]	30.9
		HT [kJ/kg]	2647
	Outlet (LP rotor outlet)	PS [barA]	0.152

Table 3 Boundary conditions for simplified and realistic domains

Results

Original Design

The performances of the original steam guide design were computed through the 3D simplified approach, which is sufficiently accurate for the complete test case in terms of the parameters under analysis, as will be demonstrated later.

Post-processing activities mostly have been carried out on the locations highlighted in Figure 5. In particular, PlaneM1 and PlaneM2 correspond to the sections where streamlines and Mach number contours will be plotted; on the other side, mass flow rate non-uniformities will be investigated on the LP stator inlet, which is divided into 10 sectors and again shown in Figure 5.

The initial design has two main features:

- An axisymmetric steam guide covers most of the axial size of the injection flanges.
- The shaft has a constant inclination throughout the whole region.

Streamlines shown in Figure 6 well represent the complex fluid dynamic structure obtained with this configuration. The injected steam flow is forced to suddenly accelerate and change direction near the guide leading edge, implying considerable total pressure losses. At the same time the flow coming from the upstream stages passes through a diffuser that lowers the axial velocity, making it more subject to the tangential component of the injected steam. This also compromises the circumferential uniformity, which promotes the recirculation below the guide. Table 4 summarizes the total pressure loss and standard deviation of the mass flow rate distribution at the LP stator inlet. The exact definition of the total pressure loss will be given in the next section, and later on, the flow rate distribution in the 10 sectors of the LP stator inlet will be compared with the final selected solution.

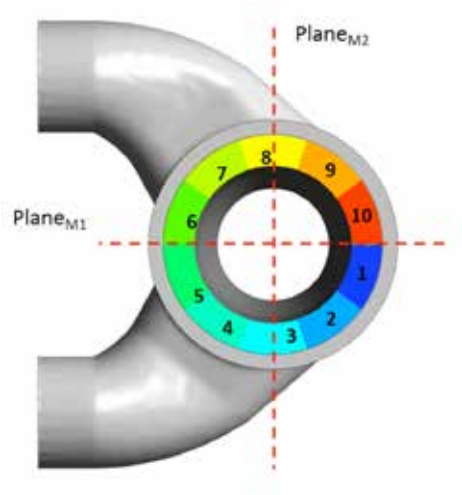

FIGURE 5 Post processing planes

Flow Rate Distribution Standard Deviation	0.41
Flow Rate Distribution Maximum Deviation	17.3%
Total Pressure Loss	8.25%

Table 4 Performances of the original configuration

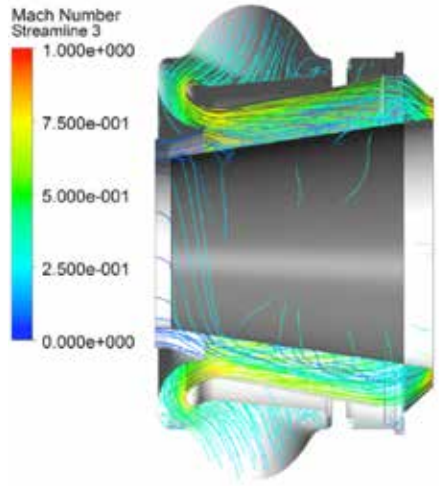

FIGURE 6A Original design: streamlines on plane$_{m1}$

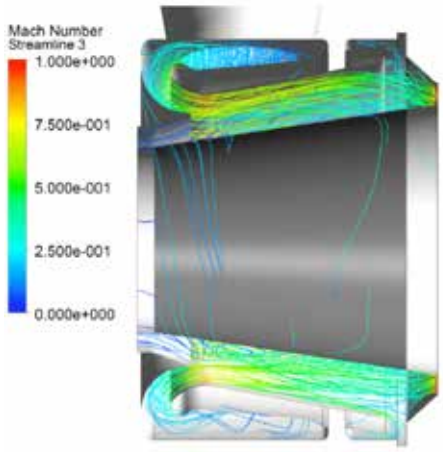

FIGURE 6B Original design: streamlines on plane$_{m2}$

Axisymmetric screening

Axisymmetric computational domain is the first step of the steam guide enhancement. This operation was performed by selecting the best solution among the DOE performed on the following four parameters illustrated in Figure 7:

- L1 and L2, concerning steam guide geometry, represent length and inclination of the guide respectively.
- Φ1 and Φ2, relative to rotor shaft geometry, are used to modify the inclination of this surface, which previously was constant in the original design.

In particular, an Optimal Space Filling DOE has been selected from the types available in ANSYS Workbench®, with the full quadratic sampling option selected to include second order cross terms as well. By changing these parameters the steam guide geometry will remain axisymmetric.

Among the parameters investigated in a previous sensitivity analysis, these two sets have had the greatest impact in terms of the objective function, which is defined as:

$$PT_{loss} = \frac{PT_{ave} - PT_{plane3}}{PT_{ave}}$$

This equation represents the total pressure loss in the LP stage inlet section, corresponding to plane 3 in Figure 7. The average total pressure PTave is evaluated as a mass-flow average between the reaction stages discharge section and injection, plane 1 and 2, respectively, according to Equation 2.

$$PT_{ave} = \frac{\dot{m}_{plane1} * PT_{plane1} + \dot{m}_{plane2} * PT_{plane2}}{\dot{m}_{plane1} + \dot{m}_{plane2}}$$

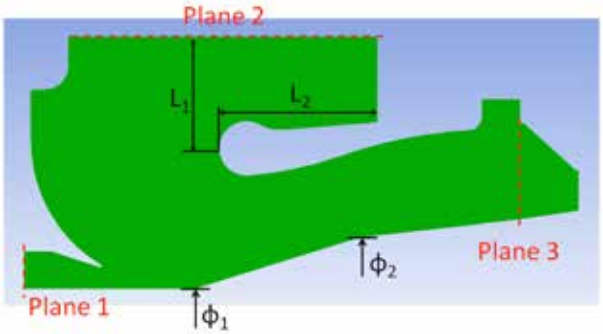

FIGURE 7 DOE parameters and post processing planes

The area restriction crossed by the upstream flow is a minor modification with respect to the original geometry, unchanged for the DOE samples. This induces a slight acceleration that makes the flow less prone to injection tangential velocity.

The results from axisymmetric CFD simulations have been employed only for selection purposes. Therefore, the minimum pressure loss achieved with this geometry, equal to 3 percent, should not be considered from a quantitative point of view. Indeed, the pressure losses later evaluated on the corresponding 3D model are noticeably higher.

In Figure 8, the contour of Mach number shows the limited maximum value achieved, below 0.4, in the most critical zone, close to the guide's leading edge. Consequently, the flow is not subject to any recirculation before the LP stator. That fact, along with the minimum pressure loss, is why the present configuration was chosen for the 3D verification.

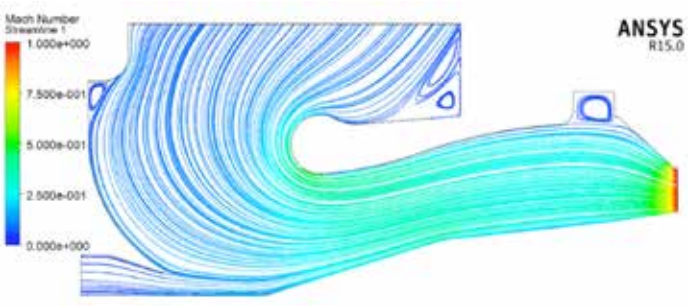

FIGURE 8 Axisymmetric geometry: Streamlines and mach number contours

Final design: 3D simplified domain

In this intermediate step, the pressure losses are verified, and the non-uniformity of the flow in the circumferential direction at the LP stage inlet is computed. Actually, a few geometries have been selected in the previous step for the simplified 3D model verification, but only the one featuring the best compromise between uniformity and losses will be discussed in the present section. First, the grid independence will be assessed by comparing total pressure loss and standard deviation of the mass flow distribution. Then the results concerning the selected geometry will be discussed further.

Grid independence: Three quantities of elements have been employed to demonstrate independence from domain discretization:

- Low – 14 million elements
- Average – 20 million elements
- High – 27 million elements.

The main parameters under analysis were used to compare the outcome of the three grids, i.e., the total pressure loss and standard deviation of the mass flow distribution at the LP stator inlet. Results, shown in Figure 9, reveal that the low level clearly overestimates both parameters, while the trend tends to flatten between the average and high levels. Therefore, the average level was considered appropriate for the following analysis, including the complete test case. Note that the average level of discretization is the same used for the original design.

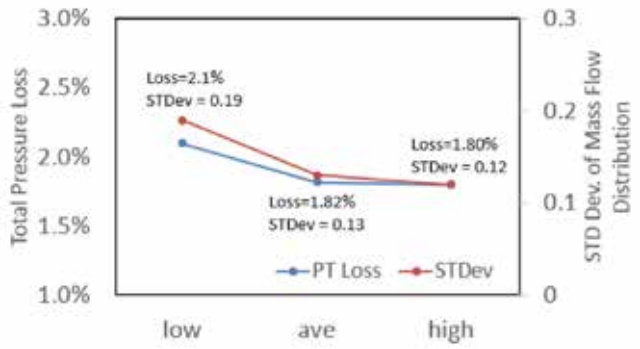

FIGURE 9 Grid independence

Performance assessment: The foremost mass flow distribution was compared with the original design. As shown in Figure 10, the higher standard deviation found for the original geometry (see Table 2), results mainly from a considerably non-uniform flow rate. This can be explained by a major impact of the injection flow, featuring a stronger tangential component that deviates the flow away from the sectors corresponding to the injection, namely 3-4 and 7-8. On the other hand, the enhanced configuration is less subject to this phenomenon; a similar trend still can be distinguished, but the peaks are much closer to the average value (black dotted line). Indeed, the maximum deviation is now acceptable since it's lower than 6 percent.

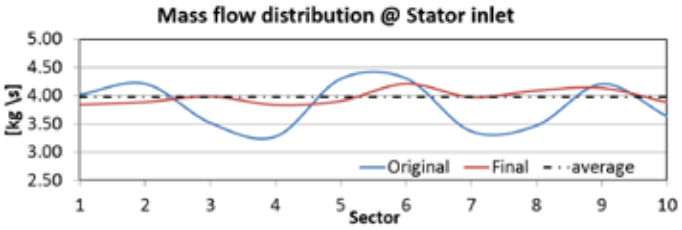

FIGURE 10 Mass flow distribution at LP stator inlet

The flow distribution also helps to explain why in Figure 11, which displays the final geometry, recirculation is present only in PlaneM2. Actually, it corresponds to the region where there is a lower portion of mass flow, sectors 3 and 4, and there is considerable tangential velocity because of the injection impact. On the other side, PlaneM1 features a well-adapted flow in the guide channel. In fact, the higher mass flow portion leads to a higher axial velocity component with respect to the destabilizing tangential one.

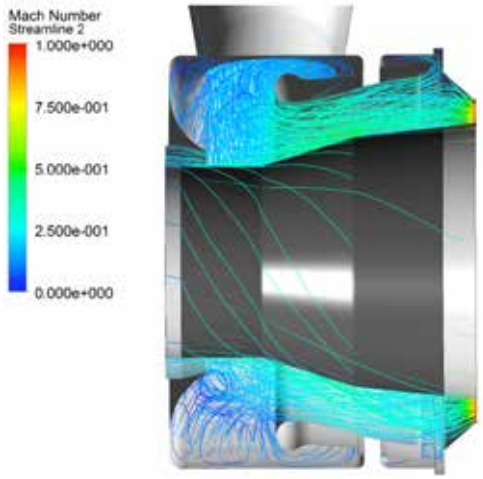

FIGURE 11 Final design: Streamlines on plane$_{m1}$

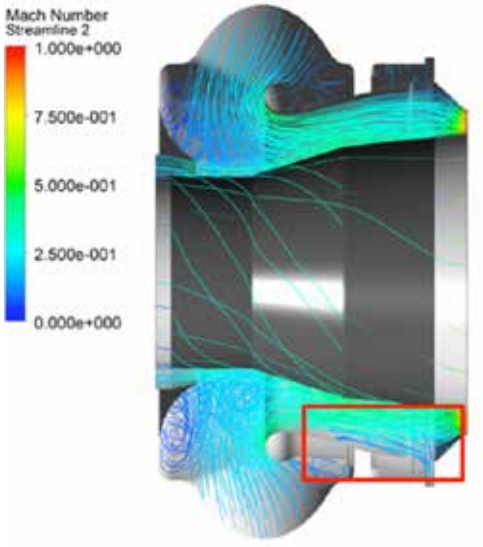

FIGURE 11 Final design: Streamlines on plane$_{m2}$

However, even with limited recirculation, the present geometry was selected to proceed with the complete test case, since it is the best compromise between flow distribution and total pressure loss at the stator inlet, which is approximately 1.82 percent.

Final design: 3D complete domain

Again, the final step is intended to more accurately assess the pressure losses and flow distribution, as well as analyze the flow uniformity at the exit of the real statoric blade row.

First, a comparison of the flow rate in the same location of the simplified geometry, i.e., the LP stator inlet, is performed, giving the distribution shown in Figure 12. The main outcome is an even better distributed flow rate in the 10 sectors under analysis. This also is demonstrated by the standard deviation and the maximum deviation—as they apply to average sector flow rate—which are almost halved in the realistic case (see Table 5). This indicates that the presence of the real blade row has a leveling impact on the flow upstream in the circumferential direction.

Moreover, the analysis of the streamlines in Figure 13 shows a better flow structure in the meridional plane, too, since the recirculation in planeM2, present in the simplified geometry, doesn't appear here.

Finally the total pressure loss, again evaluated as in Equation 1 to be coherent, is confirmed to be slightly lower than 2 percent.

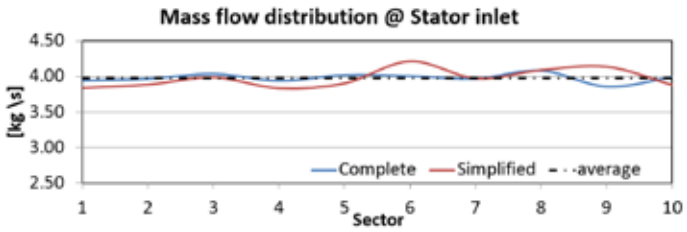

FIGURE 12 Comparison of mass flow distribution at LP stator inlet

3D MODEL	Simplified	Realistic
Flow Rate Distribution Standard Deviation	0.13	0.06
Flow Rate Distribution Maximum Deviation	5.9%	3%
Total Pressure Loss	1.82%	1.99%

Table 5 Comparison of simplified vs. realistic geometries

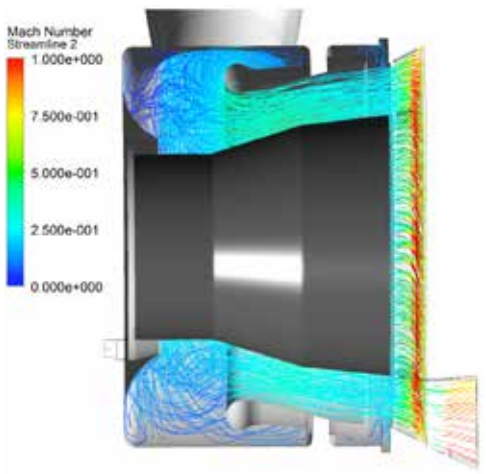

FIGURE 13 Final design, complete domain: Streamlines on plane$_{m1}$

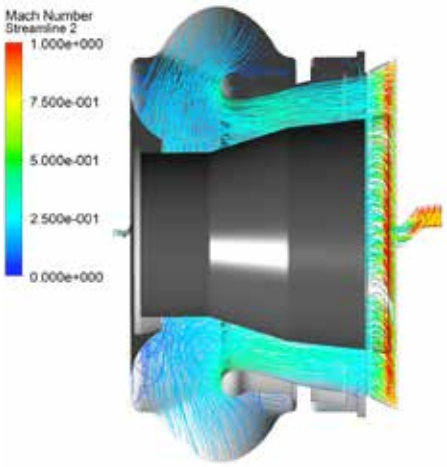

FIGURE 13 Final design, complete domain: Streamlines on plane$_{m2}$

Once the comparison between these two different approaches is completed, it is possible to discuss the flow structure at the exit of the LP stator. In particular, since the aerodynamic excitation impacting on the rotor downstream should be investigated, absolute static pressure contour was plotted, first on both the inlet and outlet plane of the LP stator. Then, the static pressure trend at three different span heights of the stator outlet was considered for the FFT analysis.

Figure 14 shows the static pressure distribution at the inlet of the stator, where the two main non-uniformities were highlighted in zones A and B. On the other side, after the expansion in the blade row, the flow distribution results displayed in Figure 15 were much more regular, with a periodic trend almost equal to the vane pitch. The lines at different span heights where the pressure signal was sampled also are shown here, while the resulting signal is illustrated in Figure 16.

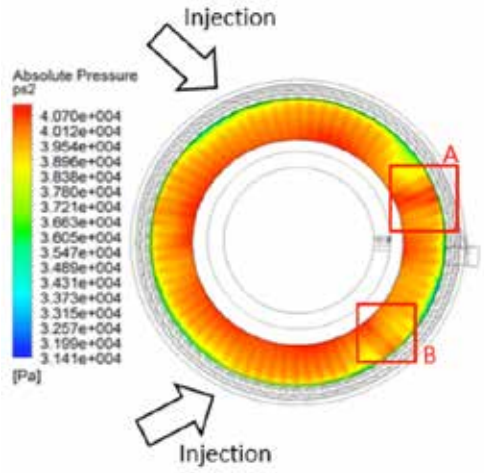

FIGURE 14 Absolute static pressure contour at lp stator inlet; non-uniformities in zones a and b

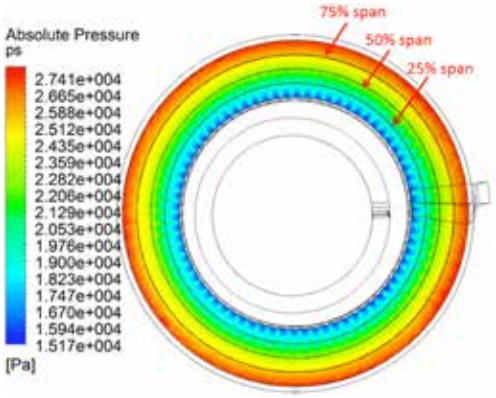

FIGURE 15 Absolute static pressure contour at LP stator outlet

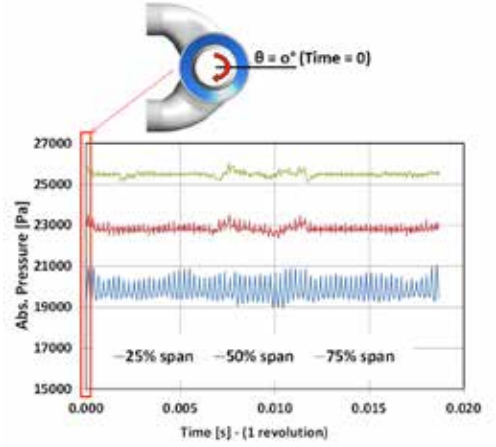

FIGURE 16 Absolute static pressure profile at 25 percent, 50 percent and 7 percent span

Note that the simulation was performed in steady state, so the time axis simply represents the time corresponding to a rotation at the given speed of 3207 RPM. Therefore, the starting time in the chart corresponds to a well-defined tangential position that also is reported in Figure 16. Obviously, the maximum time that can be defined corresponds to one complete revolution. These signals also reflect what already was stated for the pressure contour in Figure 15, namely, that no outlier peak condition can be identified, but a regular pattern was found.

Finally, the FFT analysis was carried out for each pressure signal, with the results shown in Figure 17. The NPF is found in all three cases, but at 50 percent and 75 percent of the span two more frequencies have the highest amplitude peak, 7xREV and 5xREV. However, the low peak value and the lack of corresponding natural frequencies excited in the rotor blade mean that the arising aerodynamic excitation is not dangerous for the moving blade downstream.

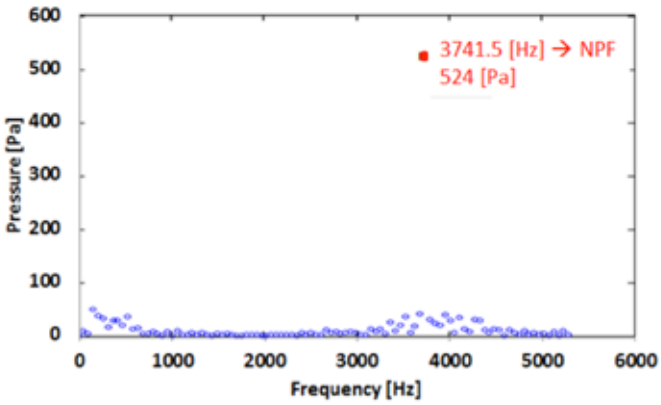

FIGURE 17A FFT analysis of pressure signal at 25 percent span

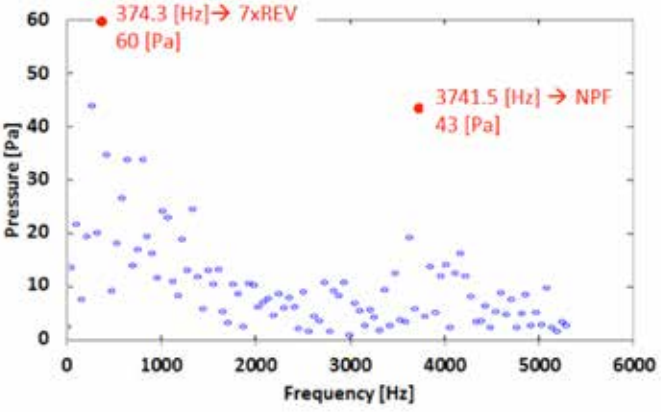

FIGURE 17B FFT analysis of pressure signal at 50 percent span

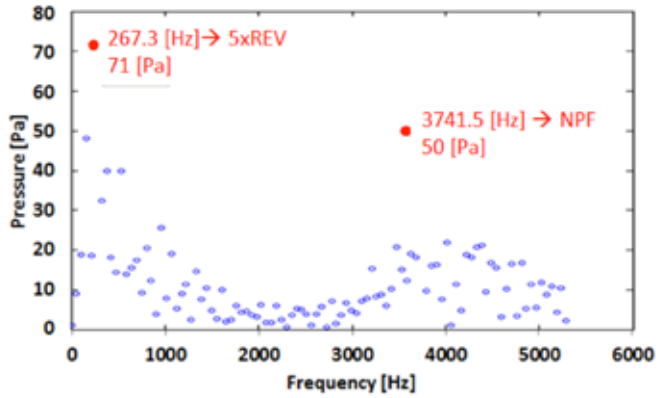

FIGURE 17C FFT analysis of pressure signal at 75 percent span

Conclusions and future work

In this study, a steam guide for a large injection system was designed to reduce total pressure loss and flow non-uniformity before the steam enters the LP stage downstream. A CFD-RANS approach was used to investigate the best solution in different steps, depending on geometry complexity.

First, the DOE analysis was performed on the axisymmetric domain by changing four different geometric parameters. Note that that losses obtained with the axisymmetric model were considered only for a qualitative assessment of the trend.

The domains that have an acceptable meridional flow structure and reduced losses were selected for the following verification by the 3D simplified model. In particular, only the final selected geometry was discussed here.

To reduce computation requirements, the 3D simplified model has a convergent duct instead of the LP stator downstream. This allowed a preliminary evaluation of the flow circumferential distribution to be performed at the inlet of the LP stator, leading to an acceptable maximum deviation of 5.9 percent. Moreover the total pressure loss obtained is approximately 1.82 percent. Both parameters were strongly reduced compared to the original design, which has a maximum deviation of 17.3 percent and a total pressure loss of 8.25 percent.

Next, the complete 3D domain, including the reaction stage upstream and LP stage downstream, was simulated to better evaluate the previous parameters and characterize the aerodynamic excitation on the LP rotor downstream. The total pressure loss is close to the value obtained with the simplified model, 1.99 percent, confirming the acceptability from this standpoint. Moreover, the flow structure became even more regular in both the meridional plane, where no recirculation is found, and the circumferential direction, with a maximum deviation halved with respect to the simplified domain. This outcome can be justified by a leveling impact of the real blade row on the flow upstream.

Finally the aerodynamic excitation at the outlet of the LP stator was computed by FFT analysis performed on pressure signal at three different span heights: 25 percent, 50 percent and 75 percent. The NPF was found, together with two additional excited frequencies. However these are not dangerous for the moving blade due to the low amplitude value and the lack of corresponding natural frequencies.

Future activities will focus on the expansion of the available steam guide geometries database for similar applications. In fact, the final purpose will be to quickly select the proper solution for given mass flow rate ratios and turbine operating conditions. Two additional points also will be investigated—the validation of the performance assessment through an experimental setup, and the evaluation of possible unsteady effects on the aerodynamic excitation.

References

1 Schramm, A., Muller, T., Polklas, T., Brunn, O. and Mailach, R., "Improvement of Flow Conditions for the Stages Subsequent to Extraction Modules in Industrial Steam Turbines", Proceedings of ASME Turbo Expo 2014 GT2014-25390.

2 Engelmann, D., Schramm, A., Polklas, T., and Mailach, R., "Losses of Steam Admission in Industrial Steam Turbines Depending on Geometrical Parameters", Proceedings of ASME Turbo Expo 2014 GT2014-25172.

3 AutoGrid5™ Documentation

4 ANSYS® CFX® 13.0 Documentation

5 Menter, F., 1993. "Zonal Two Equation k-w Turbulence Models for Aerodynamic Flows". AIAA Paper 93-2906.

6 Menter, F., Ferreira Carregal, J., Esch, T., Konno, B., 2003, "The SST Turbulence Model with Improved Wall Treatment for Heat Transfer Predictions in Gas Turbines", Proceedings of International Gas Turbine Congress IGTC2003-TS-059.

Imagination at work

GE Oil & Gas - Global Headquarters
The Ark - 201 Talgarth Road, Hammersmith - London, W6 8BJ, UK
T +44 207 302 6000
customer.service.center@ge.com

Nuovo Pignone S.p.A. - Nuovo Pignone S.r.l
Via Felice Matteucci, 2 - 50127 Florence, Italy
T +39 055 423 211
F +39 055 423 2800

Downstream Technology Solutions
4424 West Sam Houston Parkway North - Houston, TX 77041-8200, US

Enhancement of a large injection system for steam turbines
By Leonardo Nettis, Enzo Imparato, Lorenzo Cosi

GEA31926 (07/2015)